A Computational Investigation of the Geometrical Structure and Protodeboronation of Boroglycine, $H_2N-CH_2-B(OH)_2$

Joseph D. Larkin,*,†,‡ Krishna L. Bhat,§ George D. Markham,|| Bernard R. Brooks,‡ Jack H. Lai,+ and Charles W. Bock||,#

Department of Chemistry, Bloomsburg University of Pennsylvania, Bloomsburg, Pennsylvania 17815, Department of Chemistry and Biochemistry, School of Science and Health, Philadelphia University, School House Lane and Henry Avenue, Philadelphia, Pennsylvania 19144, The Institute for Cancer Research, Fox Chase Cancer Center, 333 Cottman Avenue, Philadelphia, Pennsylvania 19111, The National Institutes of Health, National Heart, Lung, and Blood Institute, Building 50, Bethesda, Maryland 20851, Department of Biochemistry, Tufts University School of Medicine, 136 Harrison Avenue, Boston, Massachusetts 02111, and Department of Chemistry, Widener University, Chester, Pennsylvania 19013

Received: January 4, 2007; In Final Form: April 16, 2007

In this article the geometrical structure of the simple, achiral, α-amino boronic acid boroglycine, $H_2N-CH_2-B(OH)_2$, was investigated using density functional theory (DFT), second-order Møller−Plesset (MP2) perturbation theory, and coupled cluster methodology with single- and double-excitations (CCSD); the effects of an aqueous environment were incorporated into the results by using a few explicit water molecules and/or self-consistent reaction field (SCRF) calculations with the IEF polarizable continuum model (PCM). Neutral reaction mechanisms were investigated for the direct protodeboronation (hydrolysis) of boroglycine ($H_2O + H_2N-CH_2-B(OH)_2 \rightarrow B(OH)_3 + H_2N-CH_3$), for which ΔH°_{298} was −21.9 kcal/mol at the MP2(FC)/aug-cc-pVDZ level, and for the 1,2-carbon-to-nitrogen shift of the $-B(OH)_2$ moiety ($H_2N-CH_2-B(OH)_2 \rightarrow H_3C-NH-B(OH)_2$), for which the corresponding value of ΔH°_{298} was −18.2 kcal/mol. A boron−oxygen double-bonded intermediate was found to play an important role in the 1,2-rearrangement mechanism.

Introduction

Although boronic acids ($R-B(OH)_2$) are not found in nature, they have emerged as an important class of compounds in chemistry, medicine, and material science,[1−4] with applications as sensors for recognizing 1,2- and 1,3-diols,[5−12] affinity ligands in chromatographic protocols,[13−17] inhibitors in serine proteases and β-lactamases,[18−20] agents in neutron capture therapy,[21,22] bioconjugates,[23] transmembrane transporters,[24−27] drugs that target the human immunodeficiency virus (HIV),[28] substrates for immobilization of proteins,[29] and submicron scale devices.[30−33] Moreover, their unique properties as mild organic Lewis acids, and their ease of handling, have made them an attractive class of synthetic intermediates,[34] and they have been widely used in Suzuki cross coupling reactions,[3] Diels−Alder reactions,[35] asymmetric synthesis of amino acids,[36] selective reduction of aldehydes,[37] and carboxylic acid activation.[38,39]

Boron analogs of amino acids present a wide array of structural diversity and they have served effectively as building blocks in combinatorial chemistry and drug discovery.[40] Such α-amino boronic acids are also precursors for the synthesis of peptide boronic acids, many of which are exceptionally potent inhibitors of serine proteases due to their ability to mimic the tetrahedral transition state binding patterns of similar carboxylic acid substrates, with increased specificity.[41−43] In fact, Bortezomib (formerly known as PS-341, and marketed as Velcade) is a novel dipeptidyl boronic acid inhibitor of the S26 proteasome that was recently approved by the FDA for the treatment of patients with relapsed multiple myeloma where the disease is refractory to conventional therapies.[44−46]

Despite the rapidly increasing use of α-amino boronic acids, many details of their geometrical structure, reactivity, and thermochemistry are not well understood.[1,47,48] In the present article, we report our results from a computational study of the simple, achiral, α-amino boronic acid boroglycine, $H_2N-CH_2-B(OH)_2$. Several derivatives of this acid, including some isoelectronic and isostructural analogs, have shown promise as chymotrypsin inhibitors,[43,49] and more recently the peptide L-γ-Gly-L-Leu-aminomethyl boronic acid has been shown to be a stronger inhibitor of glutathionyl spermidine synthetase than the phosphonic acid analog, making it an attractive target for the design of anti-parasitic drugs.[50]

In 1981, Matteson et al. were the first to report that α-amino boronic acids and esters deboronate spontaneously in protic solvents (protodeboronation) over a period of a few hours.[51] Subsequently, it was established that boronic acids and esters, bearing a tertiary amino group in the α-position, do not undergo this type of deboronation,[52,53] and that salts and acyl derivatives of amino boronic acids are stable indefinitely.[51,54,55] Indeed, the simple α-amino boronic acid, $H_2N-CH_2-B(OH)_2$, has been observed only as a TFA or HCl salt in acidic media; it deboronates within a few minutes into methylamine and boric acid when the pH of the solution rises above the pK_a of the amino group (pH ∼ 8).[56] Experimental evidence suggests that the mechanism of protodeboronation for α-amino boronic acids

* Corresponding author. Tel: (570) 389-4154. E-mail: jlarkin@bloomu.edu.
† Bloomsburg University of Pennsylvania.
‡ The National Institutes of Health.
§ Widener University.
|| Fox Chase Cancer Center.
+ Tufts University School of Medicine.
# Philadelphia University.

10.1021/jp0700682 CCC: $37.00
Published on Web 06/27/2007

and esters involves a 1,2-carbon-to-nitrogen migration of the $-B(OH)_2$ moiety initiated by a nucleophilic attack of the proximal amino group on the boron atom.[1,40,52−54,57−59] Although 1,2-rearrangements are well-established in organic chemistry, e.g., Wagner-Meerwein, pinacol-pinacolone, Hoffmann, Wulff, etc.,[60−64] to date there have been no computational studies reported in the literature on α-aminoalkylboronic acids that elucidate mechanistic aspects involved in the 1,2-shift of the $-B(OH)_2$ moiety. In this article several neutral reaction mechanisms for the protodeboronation of $H_2N-CH_2-B(OH)_2$ that yields $B(OH)_3$ and H_2N-CH_3, and for the 1,2-carbon-to-nitrogen shift of the $-B(OH)_2$ moiety that yields methylamine boronic acid, $H_3C-NH-B(OH)_2$, are compared at a variety of computational levels.

Computational Methods

Equilibrium geometries in this article were obtained using second-order Møller−Plesset perturbation theory (MP2)[65] and coupled cluster calculations with single- and double-excitations (CCSD);[66−69] the frozen core (FC) approximation was employed in all cases. The Pople 6-31G(d), 6-31+G(d) and 6-311++G(d,p)[70,71] basis sets, as well as the Dunning-Woon cc-pVDZ, cc-pCVDZ, aug-cc-pVDZ, cc-pVTZ, and aug-cc-pVTZ correlation-consistent basis sets,[72−75] were used in the calculations. Frequency analyses were performed analytically to confirm that the optimized structures were local minima on the potential energy surface (PES) and to correct reaction energies to 298 K. All calculations were performed using the GAUSSIAN 03 suite of programs.[76]

For comparison, DFT geometry optimizations were performed with the PBE1PBE functional,[77−79] which makes use of the one-parameter GGA PBE functional[77] with a 25% exchange and 75% correlation weighting. Our experience with this functional for a variety of boronic acids and esters has been that it gives results in reasonable agreement with those from second-order Møller−Plesset perturbation theory, provided that comparable basis sets are employed.[47,80−82] Since MP2 and CCSD calculations on larger α-amino boronic acids are not yet practical with high-quality basis sets, it is important to establish the reliability of specific functionals that can be employed for investigations of these increasingly important molecules.

To assess the effects of an aqueous environment, we performed self-consistent reaction field (SCRF) calculations using the IEF Polarizable Continuum Model (PCM)[83−87] as implemented in GAUSSIAN 03;[76] continuum solvent models such as IEF-PCM are an attractive alternative to explicit solvent approaches because they require less computational effort.[88] These calculations were performed at the PBE1PBE/6-311++G(d,p) and/or MP2(FC)/cc-pVDZ levels; some care must be exercised when using diffuse functions with PCM calculations as they may extend too far into the cavity region and cause instabilities in the calculation.[89] Since such PCM calculations do not incorporate specific directional aspects of protic solvents such as water,[90,91] a variety of calculations were also performed using a few explicit water molecules.

Results and Discussion

Geometrical Structure of Boroglycine, $H_2N-CH_2-B(OH)_2$. Since no experimental data are currently available on the geometrical structures of $H_2N-CH_2-B(OH)_2$, its salts, or acyl derivatives, we initially performed an extensive conformational search of this molecule at the economical PBE1PBE/6-311++G(d,p) level; various lower-energy conformers located during this search are shown in Figure 1A, along with selected geometrical parameters calculated at several, more-rigorous computational levels.

The hydroxyl groups of the lowest-energy, geometry-optimized form of $H_2N-CH_2-B(OH)_2$, **1a**, are in the so-called exo-endo orientation (see Figure 1A);[47,92−95] an intramolecular N···H−OB hydrogen bond is also present in this nonplanar conformer (τ_{OBCN} was approximately −166°), although the N···H distance was calculated to be greater than 2 Å. Computed infrared vibrational frequencies of **1a** are listed in Table 1S of the Supporting Information. The calculated B−C distance in **1a**, ∼1.59 Å, is in good agreement with the observed B−C distance of 1.588 Å in the crystal structure of 2-nitro-4-carboxyphenyl boronic acid; the $-B(OH)_2$ moiety in this crystal structure was nearly perpendicular to the phenyl ring, which minimized the bond-shortening effects of conjugation.[1,96] Geometrical structures of several additional local minima on the $H_2N-CH_2-B(OH)_2$ PES are also shown in Figure 1A; they are all higher in energy (see Table 1A). For comparison, we note that the anti form, **2a**, is less than 3 kcal/mol higher in energy than **1a**, whereas the syn form, **3a**, is greater than 6 kcal/mol higher in energy. Relative energies of conformers **1**−**3** using MP2 and CCSD methodology with the cc-pVDZ basis set exhibited a similar trend.

In the (IEF-PCM) reaction field of water conformer **1a** is also the lowest-energy conformer, but **2a** is only 0.3 and 0.2 kcal/mol higher in energy at the PBE1PBE/6-311++G(d,p) and MP2/cc-pVDZ levels respectively, significantly less than the corresponding values in vacuo; this finding is consistent with the higher calculated dipole moment of **2a**, 4.28 D, compared to that of **1a**, 1.77 D, at the PBE1PBE/6-311++G(d,p) level.

The transition state for the conversion of the exo-endo conformer **1a** of $H_2N-CH_2-B(OH)_2$ to the anti conformer **2a** via rotation about a B−O bond was relatively high in energy, e.g., 10.6 and 11.2 kcal/mol at the PBE1PBE/6-311++G(d,p) and MP2/cc-pVDZ levels respectively. The origin of this barrier is a result of the interaction of the lone pairs on the oxygen atoms with the empty p_z orbital on the tri-coordinated boron atom in **1a**, which confers partial double bond character to the B−O linkage.[1] Indeed, the length of the B−O bond in **1a** involved in the rotation increases by ∼0.03 Å in the transition state. On the other hand, the barrier for the interconversion of the two exo-endo conformers **1a** and **1b** by rotation about the B−C single bond was much lower, 5.6 and 5.7 kcal/mol at these levels; the B−C bond length does not change significantly during the rotation.

Despite repeated attempts, no local minimum on the PES that involved a 3-centered, dative-bonded (−B−C−N−) ring structure could be found in either the gas phase or in the (PCM) reaction field of water. On the other hand, the lowest-energy conformer of the analogous borane compound, $H_2N-CH_2-BH_2$, does involve a 3-centered (−B−C−N−) ring and it is 12.9 and 15.9 kcal/mol lower in energy in vacuo and in (PCM) aqueous media, respectively, than the corresponding acyclic conformer at the PBE1PBE/6-311++G(d,p) level.[97] Furthermore, this type of cyclic conformer is also a local minimum on the PES of the borinic acid analog, $H_2N-CH_2-BH(OH)$, although in this case it is 7.6 and 4.2 kcal/mol higher in energy than a conformer similar in structure to **1a**.[97] These results prompted us to search further for stable cyclic conformers of $H_2N-CH_2-B(OH)_2$ in the presence of a few explicit water molecules. Interestingly, calculations on 3-centered, dative-bonded (−B−C−N−) ring conformers of $H_2N-CH_2-B(OH)_2$, that included as many as six hydrogen-bonded water molecules, proved to be local minima at the PBE1PBE/6-311++G(d,p) level (see Figure 1S).

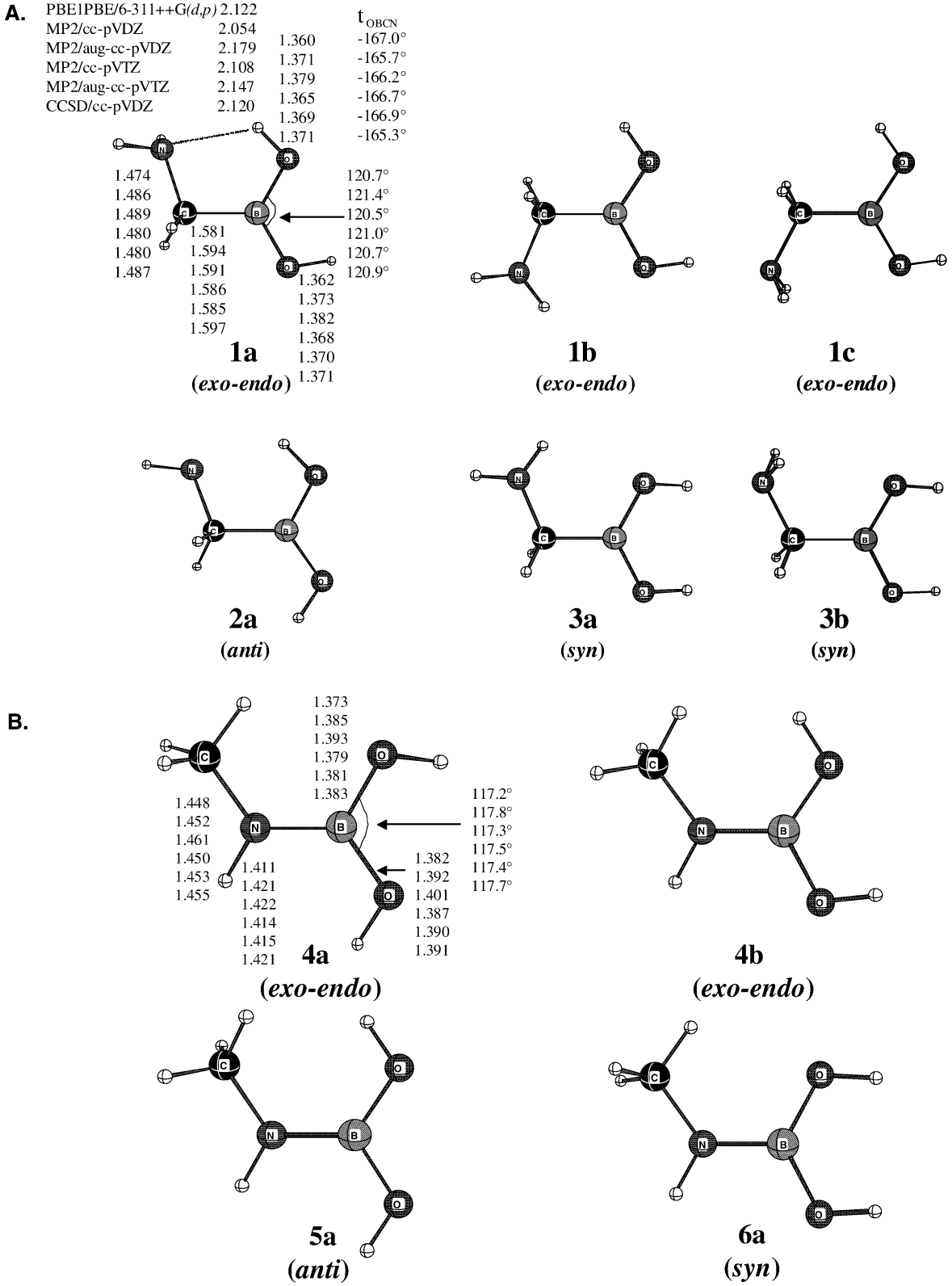

Figure 1. Optimized structures of (A) $H_2N-CH_2-B(OH)_2$ and (B) $H_3C-NH-B(OH)_2$. Distances are in Å and angles are in deg.

Although additional calculations will be required to unambiguously establish the role of such cyclic conformers in bulk water, it appears that an intramolecular nucleophilic attack of the amino group on the boron atom in $H_2N-CH_2-B(OH)_2$ is more likely in aqueous media than it is *in vacuo*.

Geometrical Structure of Methylamine Boronic Acid, $H_3C-NH-B(OH)_2$. As noted above, compounds of the form $H_2N-CHR-B(OH)_2$ may undergo a 1,2-carbon-to-nitrogen rearrangement to give the homolog $H_2RC-NH-B(OH)_2$;[1,54,58,59] thus, we investigated the geometrical structure of methylamine boronic acid, $H_3C-NH-B(OH)_2$. A selection of lower-energy conformers of this N-boryl amine are shown in Figure 1B and their relative energies are listed in Table 1B. The lowest-energy form of $H_3C-NH-B(OH)_2$, **4a,** had the hydroxyl groups in the exo-endo arrangement, similar to that found in the lowest-energy conformer of the isomer $H_2N-CH_2-B(OH)_2$; conformer **4b,** which involves a rotation about the B−N bond in **4a,** was consistently found to be less than 0.5 kcal/mol higher in energy

TABLE 1: Relative Energies, *E* (kcal/mol) (Thermally Corrected Values to 298 K in Parentheses) of Various Conformers of (A) $H_2N-CH_2-B(OH)_2$ and (B) $H_3C-NH-B(OH)_2$ at Several DFT, MP2, and CCSD Computational Levels

conf.	PBE1PBE//6-311++G(d,p)	MP2(FC)// cc-pVDZ	MP2(FC)// aug-cc-pVDZ	MP2(FC)// cc-pVTZ	MP2(FC)// aug-cc-pVTZ	CCSD(FC)// cc-pVDZ
			(A) $H_2N-CH_2-B(OH)_2$			
exo-endo						
1a	0.0 (0.0)	0.0 (0.0)	0.0 (0.0)	0.0	0.0	0.0
1b	4.3 (3.9)	5.1 (4.8)	3.6 (3.4)	4.2	3.6	4.7
1c	5.2 (5.0)	4.9 (4.7)	4.6 (4.4)	4.8	4.7	4.5
anti						
2a	2.9 (2.9)	2.7 (2.7)	2.4 (2.4)	2.4	2.3	2.8
syn						
3a	7.3 (6.8)	8.0 (7.6)	6.1 (5.7)	6.8	6.1	7.5
3b	8.3 (7.8)	8.2 (7.8)	7.3 (6.9)	7.6	7.4	7.8
			(B) $H_3C-NH-B(OH)_2$			
exo-endo						
4a	0.0 (0.0)	0.0 (0.0)	0.0 (0.0)	0.0	0.0	0.0
4b	0.3 (0.2)	0.3 (0.3)	0.4 (0.4)	0.4	0.5	0.3
anti						
5a	4.1 (3.9)	3.9 (3.8)	3.5	3.4	3.4	3.9
syn						
6a	1.8 (1.7)	1.8 (1.7)	1.5	1.6	1.4	

than **4a**. The transition state for the rotation about the B−N bond in **4a** to give **4b** is relatively high, 12.3, 10.6, and 12.0 kcal/mol at the PBE1PBE/6-311++G(d,p), MP2/cc-pVDZ, and MP2/aug-cc-pVDZ levels respectively, a result of conjugation between the nitrogen lone pair and the empty orbital p_z on the boron atom which confers partial double bond character to the B−N linkage.[1] Calculated infrared vibrational frequencies for **4a** are listed in Table 1S of the Supporting Information. In contrast to what we observed for $H_2N-CH_2-B(OH)_2$, the syn form, **6a,** of $H_3C-NH-B(OH)_2$ was lower in energy than the anti form, **5a**, presumably a result of adverse steric factors in the anti form. It must be emphasized that all of the $H_3C-NH-B(OH)_2$ conformers **4**−**6** were significantly lower in energy than the $H_2N-CH_2-B(OH)_2$ constitutional isomers **1**−**3**; e.g. **4a** was 17.8, 19.3, 19.2, 19.3, and 17.8 kcal/mol lower in energy than **1a** at the MP2/cc-pVDZ, MP2/aug-cc-pVDZ, MP2/cc-pVTZ, MP2/aug-cc-pVTZ, and CCSD/cc-pVDZ levels, respectively; the corresponding values using Pople-type basis sets at the MP2/6-31G(d), MP2/6-31+G(d), and MP2/6-311++G(d,p) levels are 19.6, 19.7, and 18.2 kcal/mol, in reasonable agreement with results using correlation-consistent basis sets. In the (PCM) reaction field of water, conformer **4a** of $H_3C-NH-B(OH)_2$ was still lowest in energy, and it was 18.2 and 18.3 kcal/mol lower in energy than conformer **1a** of $H_2N-CH_2-B(OH)_2$ at the PBE1PBE/6-311++G(d,p) and MP2/cc-pVDZ levels respectively, similar to the corresponding values in the gas phase.

Protodeboronation of $H_2N-CH_2-B(OH)_2$. In general, there is a paucity of experimental thermochemical data available in the literature for the hydrolysis of α-aminoalkylboronic acids and, to the author's knowledge, there have been no reports of quantum chemical investigations for this process. In this section we present calculated thermodynamic/kinetic data relevant to the protodeboronation of $H_2N-CH_2-B(OH)_2$.

Thermodynamic parameters for the hydrolysis reaction:

$$H_2O + H_2N-CH_2-B(OH)_2 \rightarrow B(OH)_3 + H_2N-CH_3 \qquad (1)$$

are listed at several computational levels in Table 2A. This process is predicted to be significantly exothermic in the gas phase, e.g., for conformer **1a**, the values of ΔH°_{298} are −24.2, −27.2, −21.9, and −26.3 kcal/mol at the PBE1PBE/6-311++G(d,p), MP2/cc-pVDZ, MP2/aug-cc-pVDZ, and MP2/cc-pVTZ levels, respectively, and −30.1, −27.4, and −24.0 kcal/mol at the MP2/6-31G(d), MP2/6-31+G(d), and MP2/6-311++G(d,p) levels; the importance of including diffuse functions in the basis set to accurately describe the bonding changes inherent in reaction (1) is clearly evident from these results. In the (PCM) reaction field of water, the computed value of ΔH°_{298} for this hydrolysis, −22.5 kcal/mol at the PBE1PBE/6-311++G(d,p) level, is comparable to that found in vacuo. In general, these computational results are in qualitative agreement with the available experimental observations.[57,98] In large part, the thermodynamic favorability of reaction (1) is a reflection of the difference in the strength of the B−O bond in the product, ∼124 kcal/mol, compared to of the strength of the B−C bond in the reactant, ∼77 kcal/mol.[58]

Although no experimental thermodynamic data are available for reaction 1, the enthalpy for the corresponding hydrolysis reaction of methylboronic acid, $H_3C-B(OH)_2$, has been reported to be −26.8 kcal/mol, based on published heat-of-formation data at 298 K.[58] To assess the reliability of the computational levels employed in this investigation, calculated thermodynamic data for the hydrolysis of $H_3C-B(OH)_2$ are listed in Table 3. Clearly, the computed reaction enthalpies in vacuo are in good agreement with those estimated from experimental thermochemical data. A comparison of the corresponding calculated reaction enthalpies in Tables 2A and 3 shows that the presence of a basic primary amine group in the α-position plays a rather minor role in the thermodynamics for this type of hydrolysis.

Transition state, **7a**, for the direct protodeboronation of $H_2N-CH_2-B(OH)_2$ (**1a)** is shown in Figure 2A; it involves a 4-centered ring in which the B−C distance increased by ∼0.2 Å from its value in **1a**. The rather compact geometry of the ring in **7a** is reflected in a relatively high activation barrier: $\Delta H^\ddagger$ is 36.1, 33.7, 37.0, and 34.6 kcal/mol relative to the separated reactants at the PBE1PBE/6-311++G(d,p), MP2/cc-pVDZ, MP2/aug-cc-pVDZ, and MP2/cc-pVTZ levels, respectively (see Table 2A); the corresponding values of $\Delta H^\ddagger$ using MP2 methodology with the 6-31G(d), 6-31+G(d), and 6-311++G(d,p) basis sets are similar, 37.5, 39.5, and 38.4 kcal/mol. Correction for BSSE using the counterpoise procedure raises the computed activation barrier further, e.g., by 2.2 and 6.8 kcal/mol at the PBE1PBE/6-311++G(d,p) and MP2/aug-cc-pVDZ levels, respectively. Comparing Tables 2A and 3, it is clear that the presence of a primary amino group increases the activation barrier for the protodeboronation by only ∼1−2 kcal/mol relative to the corresponding values for $H_3C-B(OH)_2$. The

TABLE 2: Thermodynamic and Kinetic Parameters (kcal/mol) for the Hydrolysis of (A)[a] $H_2N-CH_2-B(OH)_2$ and (B)[b] $H_3C-NH-B(OH)_2$

	PBE1PBE// 6-311++G(d,p)	MP2(FC)// cc-pVDZ	MP2(FC)// aug-cc-pVDZ	MP2(FC)// cc-pVTZ
		(A) $H_2N-CH_2-B(O\,H)_2$		
H_2O + **1a** → H_2N-CH_3 + $B(OH)_3$				
ΔE	−24.8	−27.9	−22.7	−27.0
ΔH°_{298}	−24.2	−27.2	−21.9	−26.3
ΔG°_{298}	−25.4	−28.5	−23.0	−27.4
H_2O + **1a** → TS**(7a)** (4-centered ring)				
$\Delta E^\ddagger$	+38.3	+35.8	+39.2	+36.8
$\Delta H^\ddagger$	+36.1	+33.7	+37.0	+34.6
$\Delta G^\ddagger$	+46.9	+44.1	+47.8	+45.3
H_2O + **1b** → TS (4-centered ring)				
$\Delta E^\ddagger$	+33.3	+31.0	+34.8	
$\Delta H^\ddagger$	+31.4	+29.0	+32.8	
$\Delta G^\ddagger$	+42.9	+40.4	+44.2	
H_2O + **2a** → TS (4-centered ring)				
$\Delta E^\ddagger$	+36.4	+33.9		
$\Delta H^\ddagger$	+34.3	+31.9		
$\Delta G^\ddagger$	+45.6	+43.2		
$2H_2O$ + **1a** → TS**(7a) (**6-centered ring)				
$\Delta E^\ddagger$	+27.1	+19.3	+28.3	
$\Delta H^\ddagger$	+26.8	+19.3	+27.8	
$\Delta G^\ddagger$	+49.1	+41.8	+49.9	
		(B) $H_3C-NH-B(OH)_2$		
H_2O + 4a → H_2N-CH_3 + $B(OH)_3$				
ΔE	−6.9	−10.2	−4.5	−7.7
ΔH°_{298}	−6.2	−9.2	−3.7	−6.9
ΔG°_{298}	−6.6	−9.5	−4.0	−7.3
H_2O + **4a** → TS**(7b)** (4-centered ring)				
$\Delta E^\ddagger$	+18.1	+12.7	+18.0	+16.0
$\Delta H^\ddagger$	+16.6	+11.3	+16.4	+14.8
$\Delta G^\ddagger$	+28.0	+22.9	+28.0	+26.0
H_2O + **4b** → TS(4-centered ring)				
$\Delta E^\ddagger$	+17.5	+12.0		
$\Delta H^\ddagger$	+16.5	+10.6		
$\Delta G^\ddagger$	+28.1	+23.3		
$2H_2O$ + **4a** → TS**(7b)** (6-centered ring)				
$\Delta E^\ddagger$	−2.1	−12.2	−2.4	
$\Delta H^\ddagger$	−2.6	−12.5	−3.3	
$\Delta G^\ddagger$	+20.0	+10.6	+19.6	

[a] $H_2O + H_2N-CH_2-B(OH)_2 \rightarrow TS \rightarrow H_2N-CH_3 + B(OH)_3$. [b] $H_2O + H_3C-NH-B(OH)_2 \rightarrow TS \rightarrow H_2N-CH_3 + B(OH)_3$.

TABLE 3: Thermodynamic and Kinetic Parameters (kcal/mol) for the Hydrolysis of $H_3C-B(OH)_2$: $H_2O + H_3C-B(OH)_2 \rightarrow TS \rightarrow CH_4 + B(OH)_3$

	PBE1PBE// 6-311++G(d,p)	MP2(FC)// 6-311++G(d,p)	MP2(FC)// cc-pVDZ	MP2(FC)// aug-cc-pVDZ	MP2(FC)// cc-pVTZ	MP2(FC)// aug-cc-pVTZ	CCSD(FC)// cc-pVDZ
			$H_2O + H_3C-B(OH)_2 \rightarrow CH_4 + B(OH)_3$				
ΔE	−28.3	−23.3	−27.7	−21.9	−31.0	−24.8	−22.4
ΔH°_{298}	−27.9	−23.0	−27.8	−21.5	−30.5	−23.9	−22.1
ΔG°_{298}	−27.1	−24.4	−25.6	−19.8	−28.3	−20.8	−20.4
			$H_2O + H_3C-B(OH)_2 \rightarrow TS \rightarrow CH_4 + B(OH)_3$				
$\Delta E^\ddagger$	+35.9	+38.8	+33.7	+37.8	+34.8	+36.6	+42.6
$\Delta H^\ddagger$	+33.7	+38.2	+33.2	+37.3	+34.2	+36.1	+42.0
$\Delta G^\ddagger$	+45.5	+49.4	+44.5	+48.6	+45.9	+48.9	+53.5

analogous activation barriers for conformers **2a** and **1b** of $H_2N-CH_2-B(OH)_2$ were similar in magnitude to that of **1a** (see Table 2A).[99,100] In the (PCM) reaction field of water, only one first-order transition state for the hydrolysis of $H_2N-CH_2-B(OH)_2$ that involved a single explicit water molecule could be located at either the PBE1PBE/6-311++G(d,p) or MP2/cc-pVDZ levels. Its geometrical structure was similar to that of **7a**; i.e. the 4-centered ring was very compact, and it was ∼40 kcal/mol higher in energy than the separated reactants.

We also located a transition state for the direct protodeboronation of **1a** using two explicit water molecules as a solvent model: it involved a 6-centered ring and the resulting activation barrier for the process was lower; e.g., the value of $\Delta H^\ddagger$ was 26.8 kcal/mol at the PBE1PBE/6-311++G(d,p) level (see Table 2A). Correction for BSSE at this level, however, raised the barrier by ∼4.0 kcal/mol, resulting in an activation enthalpy of ∼30 kcal/mol for this model. These model calculations suggest that if protodeboronation does occur directly from $H_2N-CH_2-B(OH)_2$ in aqueous media, then alternative (stepwise) mechanism(s) may exist, possibly assisted by other $H_2N-CH_2-B(OH)_2$ molecules; this possibility has not been considered in this investigation.

Protodeboronation of $H_3C-NH-B(OH)_2$. For comparison, we also calculated the corresponding thermodynamic parameters

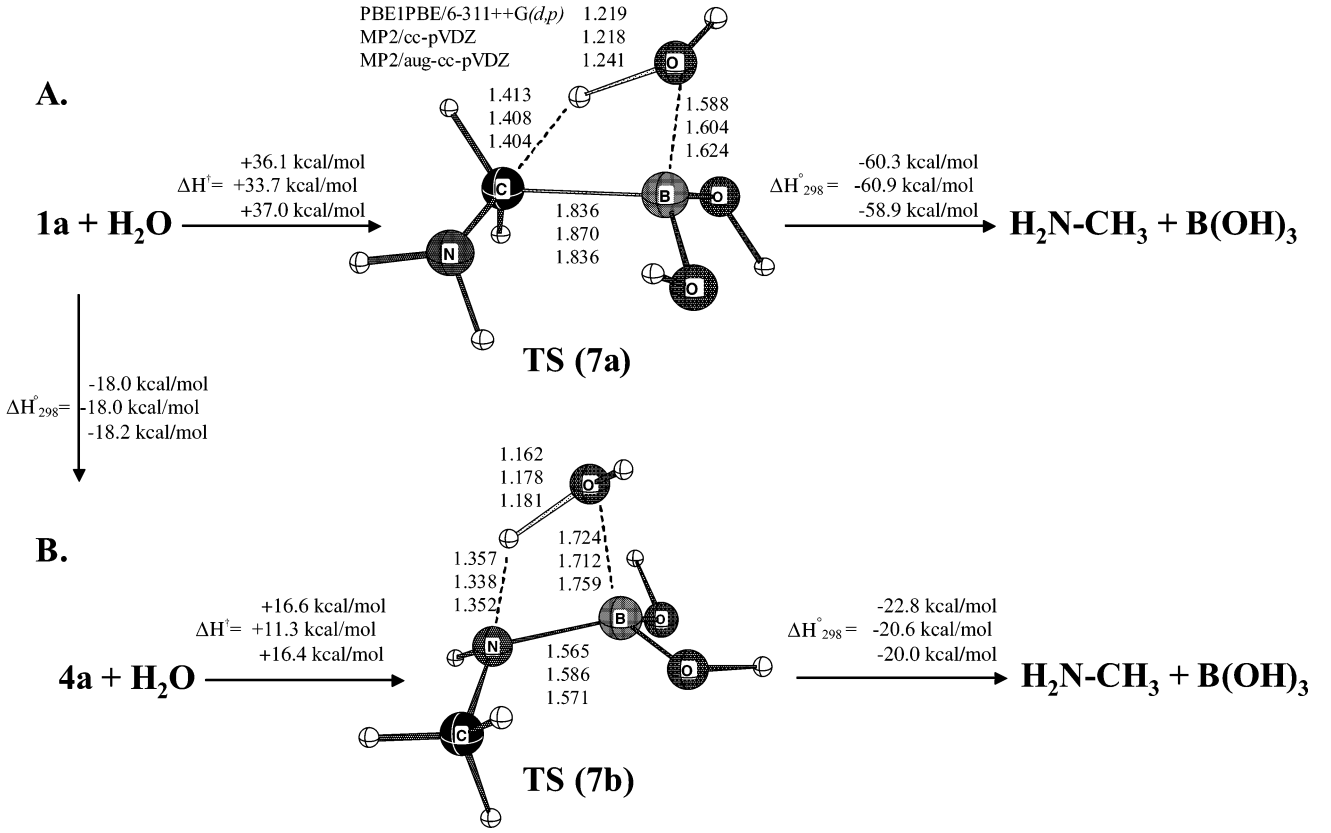

Figure 2. Optimized structures of the transition state for the direct protodeboronation of (A) $H_2N-CH_2-B(OH)_2$ (**7a**) and (B) $H_3C-NH-B(OH)_2$ (**7b**). Distances are in Å, angles are in deg, and reaction enthalpies are in kcal/mol.

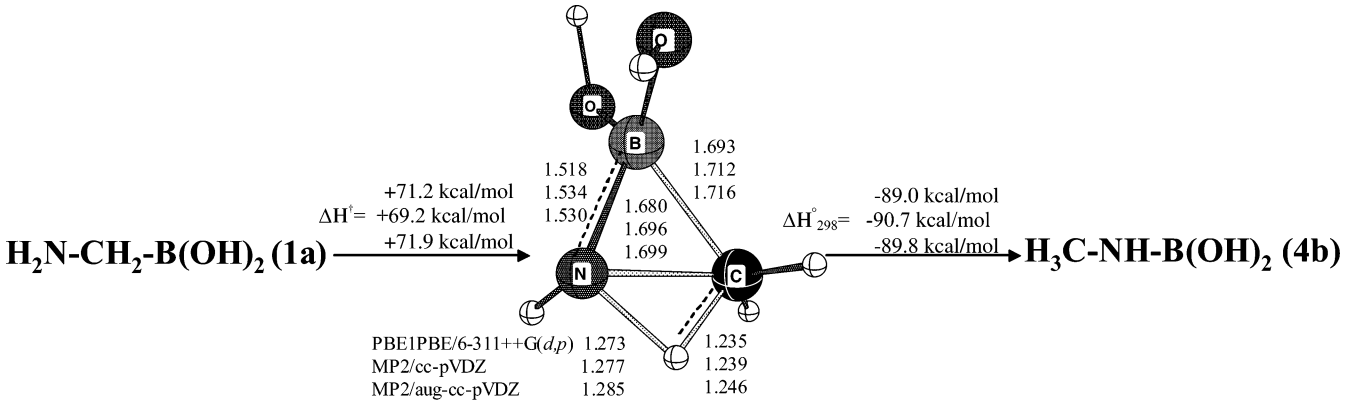

8

Figure 3. Optimized structures of the intramolecular transition state for the deboronation of $H_2N-CH_2-B(OH)_2$. Distances are in Å, angles are in deg, and reaction enthalpies are in kcal/mol.

for the hydrolysis of methylamine boronic acid, $H_3C-NH-B(OH)_2$, a constitutional isomer of boroglycine:

$$H_2O + H_3C-NH-B(OH)_2 \rightarrow B(OH)_3 + H_2N-CH_3 \qquad (2)$$

(see Table 2B). This process is also exothermic in vacuo; e.g. the calculated values of ΔH°_{298} were −6.2, −9.2, −3.7, and −6.9 kcal/mol for conformer **4a** at the PBE1PBE/6-311++G(d,p), MP2/cc-pVDZ, MP2/aug-cc-pVDZ, and MP2/cc-pVTZ levels respectively, but much less exothermic than for reaction 1 (see Table 2A); the corresponding values at the MP2/6-31G(d), MP2/6-31+G(d), and MP2/6-311++G(d,p) levels, −10.2, −7.3, and −4.9 kcal/mol, respectively, are in reasonable agreement with the higher-level calculations. In the (PCM) field of water, reaction 2 was marginally less exothermic than it was in the gas phase—the value of ΔH°_{298} was −4.1 kcal/mol at the PBE1PBE/6-311++G(d,p) level; this finding is similar to the small effect we observed for boroglycine via reaction 1.

Transition state, **7b**, for the direct protodeboronation of $H_3C-NH-B(OH)_2$ (**4a)** using one explicit water as a solvent model is shown in Figure 2B. Although the computed geometrical structure of this transition state involved a 4-centered ring similar to that of **7a**, the proton in **7b** is being transferred to a basic amine group. As a consequence, relative to the separated reactants, **4a** and H_2O, the activation enthalpy, $\Delta H^\ddagger$, was only 16.6, 11.3, 16.4, and 14.8 kcal/mol at the PBE1PBE/6-311++G(d,p), MP2/cc-pVDZ, MP2/aug-cc-pVDZ, and MP2/cc-pVTZ levels, respectively (see Table 2B), and 12.6, 16.1, and 17.8 at the MP2/6-31G(d), MP2/6-31+G(d), and MP2/6-311++G(d,p)

TABLE 4: (A) Thermodynamic and (B) Kinetic Parameters (kcal/mol) for the 1,2-Carbon-to-Nitrogen (Matteson) Rearrangement: $H_2N-CH_2-B(OH)_2 \rightarrow TS \rightarrow H_3C-NH-B(OH)_2$

	PBE1PBE//6-311++G(d,p)	MP2(FC)// cc-pVDZ	MP2(FC)// aug-cc-pVDZ	MP2(FC)// cc-pVTZ	MP2(FC)// aug-cc-pVTZ	CCSD(FC)// cc-pVDZ
(A) Thermodynamics						
1a → **4a**						
ΔE	−17.8	−17.8	−18.2	−19.2	−19.3	−17.8
ΔH°_{298}	−18.0	−18.0	−18.2	−19.4		
ΔG°_{298}	−18.8	−19.0	−19.1	−20.1		
(B) Kinetics						
1a → TS(**8**); Intramolecular						
$\Delta E^\ddagger$	+75.7	+77.6	+76.6			
$\Delta H^\ddagger$	+71.2	+69.2	+71.9			
$\Delta G^\ddagger$	+71.2	+69.0	+71.8			
1b + H_2O → TS(**9**)						
$\Delta E^\ddagger$	+27.0	+23.8	+28.2			
$\Delta H^\ddagger$	+27.0	+24.0	+28.3			
$\Delta G^\ddagger$	+38.4	+35.5	+39.4			
1a + H_2O → TS						
$\Delta E^\ddagger$	+41.3					
$\Delta H^\ddagger$	+41.1					
$\Delta G^\ddagger$	+51.2					

levels. Correction for BSSE using the counterpoise procedure raises the activation barrier by 2.1 kcal/mol for this model at the PBE1PBE/6-311++G(d,p) level and 5.9 kcal/mol at the MP2/aug-cc-pVDZ level. In the (PCM) reaction field of water, the value of $\Delta H^\ddagger$ was about 3 kcal/mol higher than in vacuo.

We also located a transition state for the protodeboronation of **4a** using two explicit water molecules as the solvent model; it involved a 6-centered ring and significantly lowered the activation barrier for the process. Indeed, the values of $\Delta H^\ddagger$ are −2.1, −12.5, and −3.3 kcal/mol at the PBE1PBE/6-311++G(d,p), MP2/cc-pVDZ, and MP2/aug-cc-pVDZ levels relative to the separated reactants (see Table 2B). The BSSE correction for this two-water model is approximately double that for the one-water model, e.g., 4.1 kcal/mol at the PBE1PBE/6-311++G(d,p) level.

Although quantitative details depend to some extent on the basis set used for the calculation and to a greater extent on the number of explicit water molecules employed, qualitatively these relatively simple solvation models suggest that protodeboronation is more facile from $H_3C-NH-B(OH)_2$ than it is from $H_2N-CH_2-B(OH)_2$.

1,2-Carbon-to-Nitrogen (Matteson) Rearrangement of the $-B(OH)_2$ Group. As noted above, compounds of the form $H_2N-CHR-B(OH)_2$ are known experimentally to undergo a 1,2-carbon-to-nitrogen migration of the $-B(OH)_2$ moiety in protic solvents.[1,40,52−54,56] In fact, the interconversion of $H_2N-CH_2-B(OH)_2$ to the isomer $H_3C-NH-B(OH)_2$ is thermodynamically favored; e.g., the calculated values of ΔH°_{298} for the conversion of **1a** to **4a** are −18.0, −18.0, −18.2, and −19.4 kcal/mol in vacuo at the PBE1PBE/6-311++G(d,p), MP2/cc-pVDZ, MP2/aug-cc-pVDZ, and MP2/cc-pVTZ levels, respectively (see Table 4A), and −19.6, −19.5, and −18.0 kcal/mol at the MP2/6-31G(d), MP2/6-31+G(d), and MP2/6-311++G(d,p) levels. The corresponding values in the (PCM) reaction field of water are also similar.

A variety of possible channels for the 1,2-migration of the $-B(OH)_2$ moiety were investigated. It should be noted that some reaction mechanisms involving 1,2-shifts have substantial activation barriers.[61−63,101] We initially considered an intramolecular rearrangement of $H_2N-CH_2-B(OH)_2$ to $H_3C-NH-B(OH)_2$ that incorporated the simultaneous transfer of a proton and the $-B(OH)_2$ group. A transition state, **8**, for this rearrangement is shown in Figure 3, and IRC analyses showed that it connects conformer **1a** of boroglycine to conformer **4b** of methylamine boronic acid. The geometrical structure of **8** involves two very compact 3-centered rings because the shared C−N distance is quite short, less than 1.70 Å. Although the boron atom is effectively 4-coordinated in **8**, the surrounding tetrahedral geometry is extremely distorted; e.g., the calculated value of the C−B−N angle was only ∼63°.[102] Consistent with these adverse geometrical features, the calculated activation barrier for this mechanism is extremely high: $\Delta H^\ddagger$ is 71.2, 69.2 and 71.9 kcal/mol above **1a** at the PBE1PBE/6-311++G(d,p), MP2/cc-pVDZ, and MP2/aug-cc-pVDZ levels, respectively (see Table 4B), and 76.1, 75.1, and 72.8 kcal/mol at the MP2/6-31G(d), MP2/6-31+G(d), and MP2/6-311++G(d,p) levels. In the (PCM) reaction field of water, **TS(8)** is also more than 70 kcal/mol higher in energy than **1a**.[90,91] Thus, any intramolecular mechanism for the isomeric conversion of $H_2N-CH_2-B(OH)_2$ to $H_3C-NH-B(OH)_2$ is not likely to be a significant pathway and this 1,2-shift apparently requires an intermolecular process.

To gain further insight into the 1,2-$B(OH)_2$-rearrangement process in an aqueous environment, we initially searched for transition states in the presence of a single explicit water molecule. Several quite different initial geometries that we employed for this shift led to transition state **TS(9)**; it involves a 7-centered ring in which the water molecule "accepts" a hydrogen bond from one of the hydroxyl groups attached to the boron atom and "donates" a hydrogen bond that appears to stabilize the emerging $-CH_2-$ moiety (see Figure 4). It is not evident from the geometry of **TS(9)** that it is involved in the 1,2-$B(OH)_2$-rearrangement process starting from boroglycine, particularly because the B−C distance is extremely long, ∼2.14 Å, and the B−N distance is quite short, ∼1.52 Å. However, IRC analyses initiated from **TS(9)** identified the corresponding reactant as the hydrogen-bonded pre-reaction **1b**···H_2O adduct shown in Figure 4. Furthermore, geometrical structures at various points along the IRC in the direction toward this adduct clearly showed the expected nucleophilic attack by the amino nitrogen atom on the boron atom via a 3-centered (−B−C−N−) cyclic geometry; indeed, the 1,2-carbon-to-nitrogen migration of the $-B(OH)_2$ moiety is clearly evident in Figure 4. Calculated values of ΔH°_{298} for the formation of this adduct from separated **1b** and H_2O are −5.7, −8.3, and −5.4 kcal/mol at the PBE1PBE/6-311++G(d,p), MP2/cc-pVDZ, and MP2/

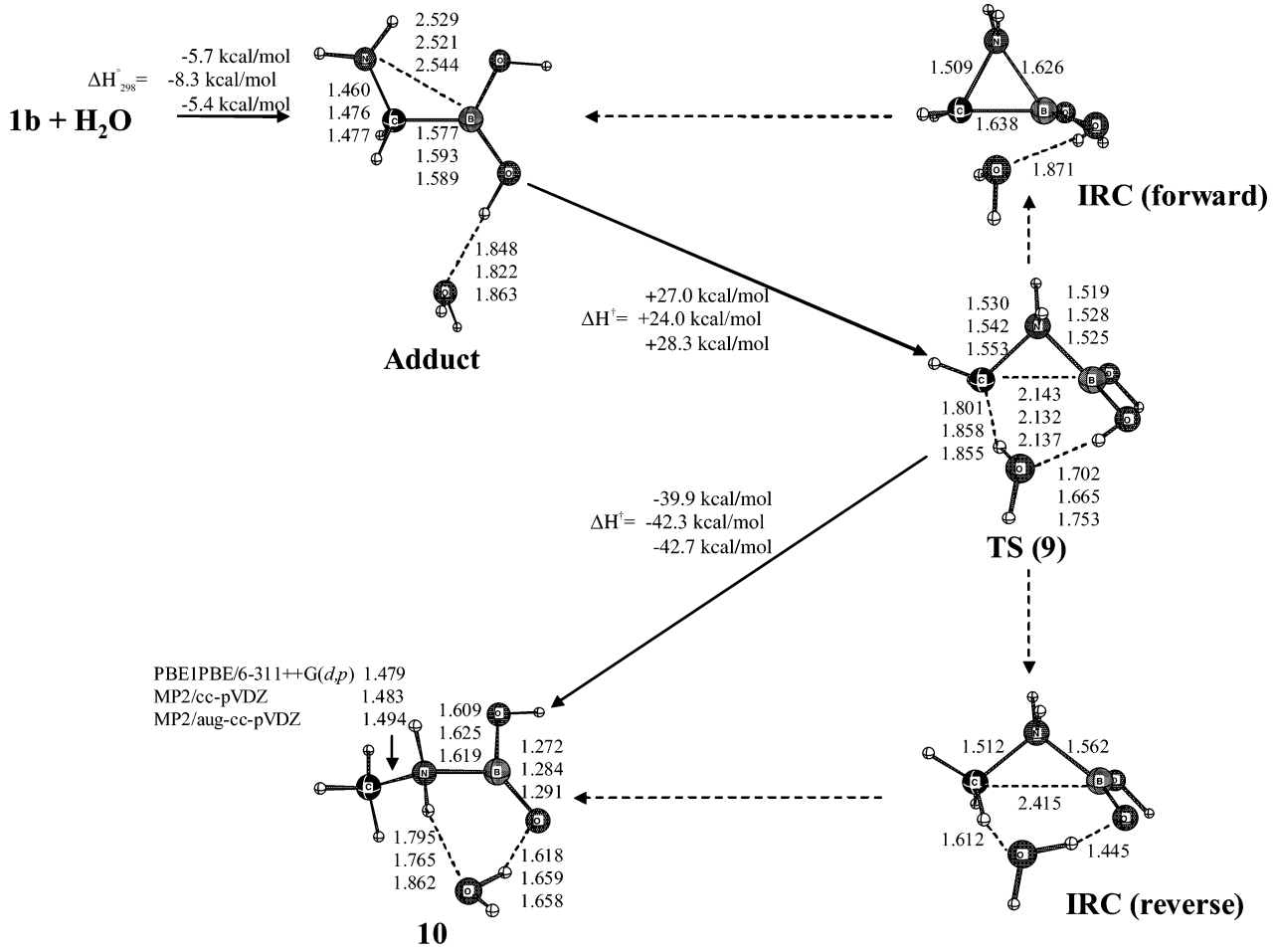

Figure 4. Reaction mechanism for the conversion of $H_2N-CH_2-B(OH)_2$ (**1b**) to the intermediate $H_3C-NH_2-B(OH)(=O)\cdots H_2O$ (**10**). Distances are in Å, angles are in deg, and reaction enthalpies are in kcal/mol.

aug-cc-pVDZ levels respectively. The predicted product of this process was a novel, monohydrated Zwitterionic intermediate, **10**, with a boron−oxygen double bond; the distance between the boron and oxygen atoms was ∼1.28 Å at the MP2/cc-pVDZ level.

The calculated activation enthalpies for the 1,2-carbon-to-nitrogen rearrangement of the $-B(OH)_2$ group *via* this one-water model are 27.0, 24.0, 28.3, 28.1, and 28.8 kcal/mol at the PBE1PBE/6-311++G(d,p), MP2/cc-pVDZ, MP2/aug-cc-pVDZ, MP2/6-31+G(d), and MP2/6-311++G(d,p) levels, respectively (see Table 4B); the corresponding value in (PCM) aqueous media at the PBE1PBE/6-311++G(d,p) level is similar. Correction for BSSE using the counterpoise procedure raised the barrier by 1.2, 8.4 and 3.0 kcal/mol at the PBE1PBE/6-311++G(d,p), MP2/cc-pVDZ, and MP2/aug-cc-pVDZ levels respectively. A transition state for the analogous conversion of **1a** and water to a B═O bonded intermediate was also located, but the associated activation barrier was substantially higher than that for **1b** (see Table 4B), as a result of steric factors in this restrictive solvation model.

Thus, the calculated activation enthalpy for the first step in the isomeric interconverion $H_2N-CH_2-B(OH)_2 \rightarrow H_3C-NH-B(OH)_2$ via the mechanism illustrated in Figure 4 (using one explicit water molecule) is ∼9 kcal/mol lower than that for the protodeboronation mechanism shown in Figure 2A; the activation enthalpies from the separated reactants are 29.3 (**TS(9)**) and 37.0 (**TS(7a)**) kcal/mol at the MP2/aug-cc-pVDZ level. For comparison, we also located one transition state for the $H_2N-CH_2-B(OH)_2 \rightarrow H_3C-NH-B(OH)_2$ interconversion using two explicit water molecules; IRC analysis showed that the reactant in this case was a hydrogen-bonded adduct involving conformer **1a** of $H_2N-CH_2-B(OH)_2$. In this solvation model the activation enthalpy, 19.7 kcal/mol at the MP2/aug-cc-pVDZ level, was ∼8 kcal/mol lower than the corresponding two-water direct protodeboronation mechanism. The predicted product from an IRC analysis of this process was similar to **10** in that it involved a boron-oxygen double bond.

Keeping in mind that the models employed in this study are very simple, these calculations suggest that the barrier for the conversion of $H_2N-CH_2-B(OH)_2$ to $H_3C-NH-B(OH)_2$ is lower than the barrier for the direct protodeboronation of $H_2N-CH_2-B(OH)_2$.

The boron-oxygen doubly bonded intermediate **10** merits some discussion. The length of the B═O bond in **10** was computed to be only 1.27, 1.28, and 1.29 Å in vacuo at the PBE1PBE/6-311++G(d,p), MP2/cc-pVDZ, and MP2/aug-cc-pVDZ levels, respectively (the B−O(H) bond length in **10** is much longer, 1.39, 1.40, and 1.41 Å, respectively), and NBO analyses indicate the presence of double bond. The calculated values of ΔH°_{298} for the formation of **10** from separated **1b** and H_2O are −12.9, −18.4, and −14.4 kcal/mol at these levels. Although there has been some evidence for the intermediacy of such boron-oxygen double-bonded structures, Vidovic et al.[103] recently prepared and structurally characterized (via X-ray crystallography) a stable Lewis acid-coordinated oxoborane compound in which the boron-oxygen functionality retained significant double bond character. Intermediate **10** was also found to be a local minimum in the reaction field of water at

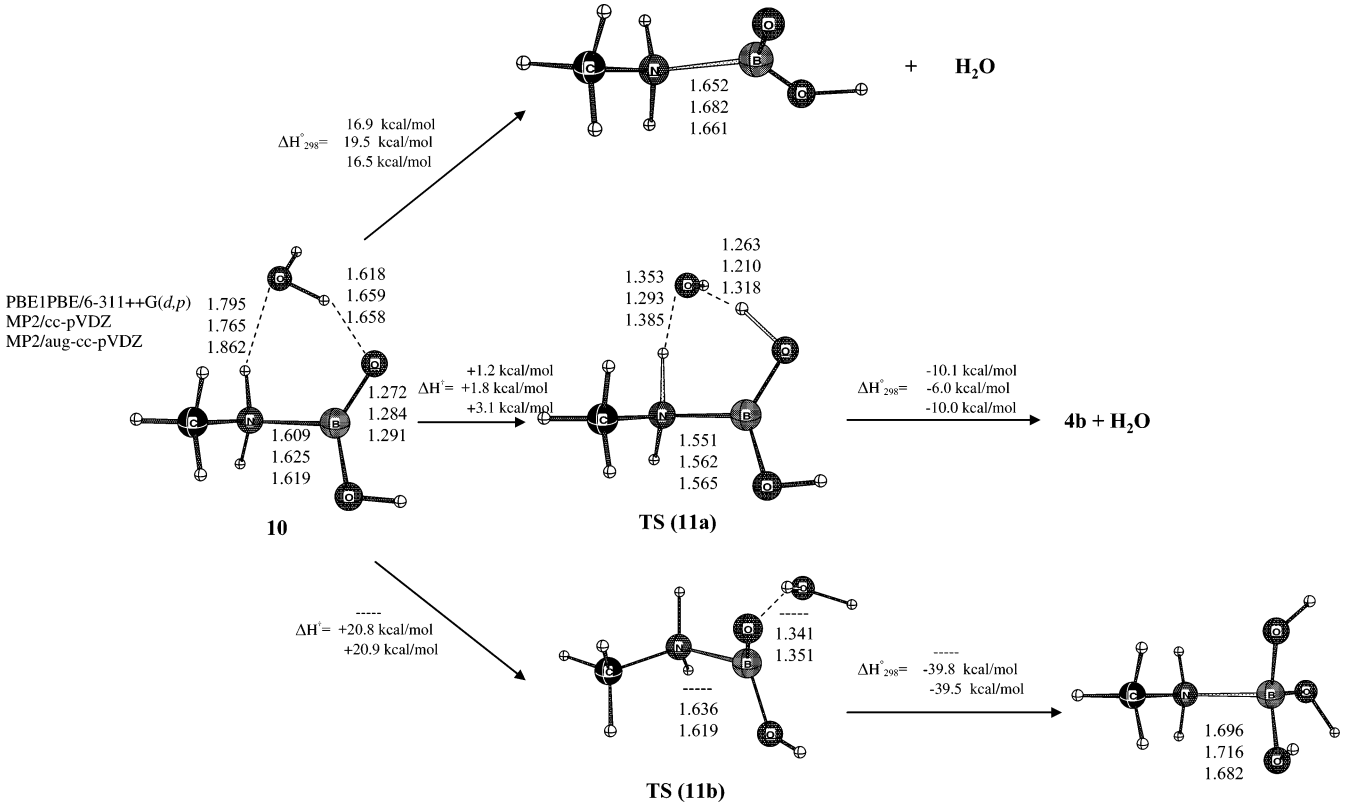

Figure 5. Reaction mechanisms for the decomposition of intermediate $H_3C-NH_2-B(OH)(=O)\cdots H_2O$(10). Distances are in Å, angles are in deg, and reaction enthalpies are in kcal/mol.

both the PBE1PBE/6-311++G(d,p) and MP2/cc-pVDZ levels, where the calculated boron-oxygen distances were 1.29 and 1.30 Å respectively.[104] To the authors knowledge, there has been no experimental evidence to suggest that a boron−oxygen, double-bonded structure plays any role in the 1,2-$B(OH)_2$-migration process.

Reactions of Intermediate (10). Several possible dissociation routes for intermediate **10** were investigated (see Figure 5). First, removing the water molecule from **10** requires a significant amount of energy: the calculated values of ΔH°_{298} are 16.8, 19.5, and 16.5 kcal/mol at the PBE1PBE/6-311++G(d,p), MP2/cc-pVDZ, and MP2/aug-cc-pVDZ levels, respectively (see Table 5A); the corresponding values at the MP2/6-31G(d) and MP2/6-31+G(d) levels are 18.6 and 16.8 kcal/mol. In the reaction field of water the values for this dissociation were significantly lower, 7.9 and 12.9 kcal/mol at the PBE1PBE/6-311++G(d,p) and MP2/cc-pVDZ levels, respectively.

Next, a proton-transfer transition state **11a** was located; IRC analyses showed that it connects **10** to a $H_3C-NH-B(OH)_2$-(**4b**)$\cdots H_2O$ adduct which was ∼12 kcal/mol lower in energy. The calculated activation enthalpies, $\Delta H^\ddagger$, for this pathway from **10** were quite low; only 1.2, 1.8, and 3.1 kcal/mol was at the PBE1PBE/6-311++G(d,p), MP2/cc-pVDZ, and MP2/aug-cc-pVDZ levels, respectively (see Table 5B). In the reaction field of water, **11a** was 10.2 kcal/mol higher in energy than **10** at the MP2(FC)/cc-pVDZ level.

Intermediate **10** is an isomer of the dative-bonded structure $H_3C-H_2N{:}B(OH)_3$, and the interconversion: **10** → $H_3C-H_2N{:}B(OH)_3$, is thermodynamically favorable − the value of ΔH°_{298} is approximately −19.0 kcal/mol (see Table 5A). The transition state for this process **11b** was located (see Figure 5), and the calculated activation enthalpies for this pathway from intermediate **10** were 20.8 and 20.9 kcal/mol at the MP2/cc-pVDZ and MP2/aug-cc-pVDZ levels, significantly higher than that required for the dissociation of **10** into $H_3C-NH_2-B(OH)(=O)$ and H_2O.[105]

Thus, of the simple model dissociation mechanisms we investigated for the decomposition of intermediate **10,** the lowest activation barrier is for its conversion to an $H_3C-NH-B(OH)_2$-(**4b**)$\cdots H_2O$ adduct.[106]

TABLE 5: (A) Thermodynamic and (B) Kinetic Parameters (kcal/mol) for Reactions of Intermediate 10

		MP2(FC)	
	PEB1PBE//6-311++G(p,d)	cc-pVDZ	aug-cc-pVDZ
(A) Thermodynamics			
10 → **4b** + H_2O			
ΔE	−6.5	−1.6	−4.4
ΔH°_{298}	−8.9	−4.2	−6.9
ΔG°_{298}	−19.0	−15.5	−17.0
10 → $H_3C-NH_2-B(OH)(=O)$ + H_2O			
ΔE	+18.4	+21.4	+18.1
ΔH°_{298}	+16.8	+19.5	+16.5
ΔG°_{298}	+6.9	+9.0	+5.9
10 → $H_3C-H_2N{:}B(OH)_3$			
ΔE	−19.1	−18.7	−18.5
ΔH°_{298}	−19.0	−19.0	−18.6
ΔG°_{298}	−17.7	−18.1	−17.6
(B) Kinetics			
10 → TS(**11a**)			
$\Delta E^\ddagger$	+5.5	+6.4	+7.6
$\Delta H^\ddagger$	+1.2	+1.8	+3.1
$\Delta G^\ddagger$	+2.9	+3.2	+4.8
10 → TS(**11b**)			
$\Delta E^\ddagger$		+23.9	+24.1
$\Delta H^\ddagger$		+20.8	+20.9
$\Delta G^\ddagger$		+22.0	+22.3

Concluding Remarks

Boronic acids have emerged as an important class of compounds in chemistry, medicine, and material science.[1−4] In this article we have described our computational findings for 1) a variety of conformers of the simple, achiral, α-amino boronic acid $H_2N-CH_2-B(OH)_2$ and its constitutional isomer $H_3C-NH-B(OH)_2$, 2) neutral protodeboronation mechanisms of $H_2N-CH_2-B(OH)_2$ and $H_3C-NH-B(OH)_2$ that yield boric acid $B(OH)_3$ and methylamine, and 3) neutral 1,2-carbon-to-nitrogen (Matteson) rearrangement mechanisms of $H_2N-CH_2-B(OH)_2$ that yield $H_3C-NH-B(OH)_2$. The calculations were carried out in the gas phase, in the presence of a few explicit water molecules, and/or in the reaction field of water.

In general, there was excellent agreement among the PBE1PBE/6-311++G(d,p), MP2/(aug)-cc-pVDZ, MP2/(aug)-cc-pVTZ, and CCSD/cc-pVTZ levels employed in this investigation as to the relative energies of various conformers of $H_2N-CH_2-B(OH)_2$ and $H_3C-NH-B(OH)_2$ (see Table 1). When diffuse functions were included in the basis set, calculated reaction thermodynamics/kinetics associated with $H_2N-CH_2-B(OH)_2$ were also in good agreement; indeed, the more economical split-valence Pople-type 6-31+G(d) and 6-311++G(d,p) basis sets performed reasonably well in this investigation compared to the more-complete and correlation-consistent basis sets we employed. The isomeric interconversion, $H_2N-CH_2-B(OH)_2$ (**1a**) → $H_3C-NH-B(OH)_2$ (**4a**), was predicted to be significantly exothermic at all levels, e.g., $\Delta H^\circ_{298} = -18.2$ kcal/mol at the MP2/aug-cc-pVDZ level, as was the overall hydrolysis: $H_2O + H_2N-CH_2-B(OH)_2$ (**1a**) → $B(OH)_3 + H_2N-CH_3$, e.g. $\Delta H^\circ_{298} = -21.9$ kcal/mol at the same level.[1,98] The activation barrier for the direct protodeboronation of $H_2N-CH_2-B(OH)_2$ (**1a**) was found to be quite high, $\Delta H^\ddagger = 37.0$ (one explicit water molecule) and 27.8 (two explicit water molecules) kcal/mol relative to the isolated reactants at the MP2/aug-cc-pVDZ level; the corresponding values for $H_3N-NH-B(OH)_2$(**4a**) were much lower, 16.4 and −3.3 kcal/mol. The barrier for the 1,2-carbon-to-nitrogen rearrangement of the $-B(OH)_2$ group from boroglycine was lower than that for the protodeboronation, $\Delta H^\ddagger = +28.3$ (one explicit water molecule) and 19.7 (two explicit water molecules) kcal/mol; IRC analyses showed that the product of the 1,2-shift was a novel hydrogen-bonded Zwitterionic intermediate with a boron-oxygen double bond.[103] The lowest-energy pathway for the disposition of this intermediate that we found involved a proton-transfer that yielded a monohydrated adduct of $H_3C-NH-B(OH)_2$.

Some caution must be exercised in extrapolating our computed results for simple model systems to experimental, aqueous-based α-amino boronic acid chemistry. Nevertheless, these calculations support observations that a 1,2-carbon-to-nitrogen shift of the $-B(OH)_2$ group is a mechanistic feature of this chemistry that must be considered. Molecular dynamics (MD) simulations of simple α-amino boronic acids, such as $H_2N-CH_2-B(OH)_2$, in aqueous media are sorely needed to compliment the investigation presented in this article. Unfortunately, values for many of the molecular mechanics (MM) parameters required for accurate MD simulations are not available and, in any event, those parameters that are available must be updated in view of recent developments.[107−110] Additional experimental and *ab initio* studies of α-amino, boronic-acid systems are also necessary to establish a more extensive database from which to determine reliable parameters for such MD simulations.

Acknowledgment. This research was supported in part by the Intramural Research Program of the NIH, NHLBI. K.L.B. would like to thank the National Textile Center (C03-PH01), and G.D.M. would like to thank the NIH (GM31186, CA06927) and NCI for financial support of this work, which was also supported by an appropriation from the Commonwealth of Pennsylvania.

Supporting Information Available: Table 1S: vibrational frequencies (cm^{-1}) of $H_2N-CH_2-B(OH)_2$ (**1a**) and $H_3C-NH-B(OH)_2$ (**4a**) calculated at the MP(2)/aug-cc-pVDZ computational level. Figure 1S: optimized structure of a stable cyclic conformer of $H_2N-CH_2-B(OH)_2$ in the presence of six hydrogen-bonded water molecules at the PBE1PBE/6-311++G(d,p) computational level. This material is available free of charge via the Internet at http://pubs.acs.org.

References and Notes

(1) Hall, D. G. *Boronic Acids*; Wiley-VCH Verlag: Weinheim, Germany, 2005.

(2) Yang, W.; Gao, X.; Wang, B. Boronic acid compounds as potential pharmaceutical agents. *Med. Res. Rev.* **2003**, *23*, 346−368.

(3) Miyaura, N.; Suzuki, A. Palladium-catalyzed cross-coupling reactions of organoboron compounds. *Chem. Rev.* **1995**, *95*, 2457−2483.

(4) Suzuki, A. *Metal-catalyzed Cross-coupling Reactions*; Wiley-VCH: Weinheim, Germany, 1998.

(5) Franzen, S.; Ni, W.; Wang, B. Study of the mechanism of electron-transfer quenching by boron-nitrogen adducts in fluorescent sensors. *J. Phys. Chem. B* **2003**, *107*, 12942−12948.

(6) Koumoto, K.; Takenchi, M.; Shinkai, S. Design of visualized sugar sensing system utilizing a boronic acid-azopyridine interaction. *Supramol. Chem.* **1998**, *9*, 203.

(7) Ni, W.; Fang, H.; Springsteen, G.; Wang, B. The design of boronic acid spectroscopic reporter compounds by taking advantage of the pK(a)-lowering effect of diol binding: nitrophenol-based color reporters for diols. *J. Org. Chem.* **2004**, *69*, 1999−2007.

(8) Otsuka, H.; Uchimura, E.; Koshino, H.; Okano, T.; Kataoka, K. Anomalous binding profile of phenylboronic acid with N-acetylneuraminic acid (Neu5Ac) in aqueous solution with varying pH. *J. Am. Chem. Soc.* **2003**, *125*, 3493−3502.

(9) Philips, M. D.; James, T. D. Boronic acid based modular fluorescent imaging of glucose. *J. Fluores.* **2004**, *14*, 549−559.

(10) Springsteen, G.; Wang, B. A detailed examination of boronic acid-diol complexation. *Tetrahedron* **2002**, *58*, 5291−5300.

(11) Steiegler, S. Selective carbohydragte recognition by synthetic receptors in aqueous solution. *Curr. Org. Chem.* **2003**, *7*, 81−102.

(12) Wang, W.; Gao, X.; Wang, B. Boronic-acid based sensors for carbohydrates. *Curr. Org. Chem.* **2002**, *6*, 1285−1317.

(13) Li, X.-C.; Scouten, W. H. New ligands for boronate affinity chromatography. *J. Chromatogr., A* **1994**, *687*, 61−69.

(14) Wulff, G. Molecular imprinting in cross-linked materials with the aid of molecular templates-a way towards artificial. *Angew. Chem., Int. Ed. Engl.* **1995**, *34*, 1812−1832.

(15) Westmark, P. R.; Valencia, L. S.; Smith, B. D. Influence of eluent anions in boronate affinity chromatography. *J. Chromatogr., A* **1994**, *664*, 123−128.

(16) Liu, G.; Hubbard, J. L.; Scouten, W. H. Synthesis and structural investigation of two potential boronate affinity chromatography ligands catechol [2-(diethylamino)carbonyl, 4-methyl]phenylborante. *J. Organomet. Chem.* **1995**, *493*, 91−94.

(17) Psotova, L. Boronate affinity-chromatography and the ap. *Chem. Listy* **1995**, *89*, 641−648.

(18) Di Costanzo, L.; Sabio, G.; Mora, A.; Rodriguez, P. C.; Ochoa, A.C.; Centeno, F.; Christianson, D. W. Crystal structure of human arginase I at 1.29-angstrom resolution and exploration of inhibition in the immune response. *Proc. Natl. Acad. Sci. U.S.A.* **2005**, *102*, 13058−13063.

(19) Benini, S.; Rypniewski, W. R.; Wilson, K. S.; Mangani, S.; Ciurli, S. Molecular details of urease inhibition by boric acid: insights into the catalytic mechanism. *J. Am. Chem. Soc.* **2004**, *126*, 3714−3715.

(20) Chen, Y.; Shoichet, B.; Bonnet, R. Structure, function, and inhibition along the reaction coordinate of CTX-M beta-lactamases. *J. Am. Chem. Soc.* **2005**, *127*, 5423−5434.

(21) Shull, B. K.; Spielvogel, D. E.; Gopalaswamy, R.; Sankar, S.; Boyle, P. D.; Head, G.; Devito, K. Evidence for spontaneous, reversible paracyclophane formation. Aprotic solvation structure of the boron neutron capture therapy drug, L-P-boronophenylaline. *J. Chem. Soc., Perkin Trans.* **2000**, *2*, 557−561.

(22) Srivastava, R. R.; Singhaus, R. R.; Kabalka, G. W. 4-Dihydroxyborylphenyl analogues of 1-aminocyclobutanecarboxylic acids: potential boron neutron capture therapy agents. *J. Org. Chem.* **1999**, *64*, 8495−8500.

(23) Stolowitz, M. L.; Ahlem, C.; Hughes, K. A.; Kaiser, R. J.; Kesicki, E. A.; Li, G.; Lund, K. P.; Torkelson, S. M.; Wiley, J. P. Phenylboronic acid-salicylhydroxamic acid bioconjugates. 1. A novel boronic acid complex for protein immobilization. *Bioconjugugate Chem.* **2001**, *12*, 229−239.

(24) Paugam, M.-F.; Bien, J. T.; Smith, B. D.; Chrisstoffels, L. A. J.; deJong, F.; Reinhoudt, D. N. Facilitated catecholamine transport through bulk and polymer-supported liquid membranes. *J. Am. Chem. Soc.* **1996**, *118*, 9820−9825.

(25) Duggan, P. J. Fructose-permeable liquid membranes containing boronic acid carriers. *Aust. J. Chem.* **2004**, *57*, 291−299.

(26) Smith, B. D. Advances in Supramolecular Chemistry. (Gokel, G.W., ed.), vol. 5, pp. 157−202. JAI Press 1999.

(27) Westmark, P. R.; Gardiner, S. J.; Smith, B. D. Selective monosaccharide transport through lipid bilayers using boronic acid carriers. *J. Am. Chem. Soc.* **1996**, *118*, 11093−11100.

(28) Chen, Y.; Bastow, K. F.; Goz, B.; Kucera, L.; Morris-Natschke, S. L.; Ishaq, K. S. Boronic acid derivatives targeting HIV-1. *Antiviral Chem. Chemother.* **1996**, *7*, 108−114.

(29) Frantzen, F.; Grimsrud, K.; Heggli, D. E.; Sundrehagen, E. Soluble highly coloured phenylboronic acids and their use in glycohemoglobin quantification. *Clin. Chim. Acta* **1997**, *263*, 207−224.

(30) Li, Y.; Ruoff, R. S.; Chang, R. P. H. Boric acid nanotubes, nanotips, nanorods, microtubes, and microtips. *Chem. Mater.* **2003**, *15*, 3276−3285.

(31) Wang, W.; Zhang, Y.; Huang, K. Prediction of a family of cage-shaped boric acid clusters. *J. Phys. Chem. B* **2005**, *109*, 8562−8564.

(32) Wang, W.; Zhang, Y.; Huang, K. Self-curl and self-assembly of boric acid clusters. *Chem. Phys. Lett.* **2005**, *405*, 425−428.

(33) Parry, P. R.; Wang, C.; Batsanov, A. S.; Bryce, M. R.; Tarbit, B. Functionalized pyridylboronic acids and their Suzuki cross-coupling reactions to yield novel heteroarylpyridines. *J. Org. Chem.* **2002**, *67*, 7541−7543.

(34) Ferrier, R. J. Carbohydrate boronates. *Adv. Carbohydrate Chem. Biochem.* **1978**, *35*, 31−80.

(35) Ishihara, K.; Yamamoto, H. Arylboron compounds as acid catalysts in organic synthetic transformations. *Eur. J. Org. Chem.* **1999**, 527−538.

(36) Petasis, N. A.; Zavialov, I. A. A new and practical synthesis of alpha-amino acids from alkenyl boronic acids. *J. Am. Chem. Soc.* **1997**, *119*, 445−446.

(37) Yu, H.; Wang, B. Phenylboronic acids facilitated selective reduction of aldehydes by tributyltin hydride. *Synth. Commun.* **2001**, *31*, 163−169.

(38) Latta, R.; Springsteen, G.; Wang, B. Development and synthesis of an arylboronic acid-based solid-phase amidation catalyst. *Synthesis* **2001**, 1611−1613.

(39) Yang, W.; Gao, X.; Springsteen, G.; Wang, B. Catechol pendant polystyrene for solid-phase synthesis. *Tetrahedron Lett.* **2002**, 6339−6342.

(40) Dembitsky, V. M.; Srebnik, M. Synthesis and biological activity of alpha-aminoboronic acids, amine-carboxyboranes and their derivatives. *Tetrahedron* **2003**, *59*, 579−593.

(41) Ivanov, D.; Bachovchin, W. W.; Redfield, A. G. Boron-11 pure quadrupole resonance investigation of peptide boronic acid inhibitors bound to alpha-lytic protease. *Biochemistry* **2002**, *41*, 1587−1590.

(42) Jagannathan, S.; Forsyth, T. P.; Kettner, C. A. Synthesis of boronic acid analogues of alpha-amino acids by introducing side chains as electrophiles. *J. Org. Chem.* **2001**, *66*, 6375−6380.

(43) Dembitsky, V. M.; Quntar, A. A.; Srebnik, M. Recent advances in the medicinal chemistry of alpha-aminoboronic acids, amine-carboxyboranes and their derivatives. *Mini Rev. Med. Chem.* **2004**, *4*, 1001−1018.

(44) Adams, J.; Behnke, M.; Chen, S.; Cruickshank, A. A.; Dick, L. R.; Grenier, L.; Klunder, J. M.; Ma, Y. T.; Plamondon, L.; Stein, R. L. Potent and selective inhibitors of the proteasome: dipeptidyl boronic acids. *Bioorg. Med. Chem. Lett.* **1998**, *8*, 333−338.

(45) Labutti, J.; Pearsons, I.; Huang, R.; Miwa, G.; Gan, L.-S.; Daniels, J. S. Oxidative deboronation of the peptide boronic acid proteosome inhibitor bortezomib: contributions from reactive oxygen species in this novel cytochrome P450 reaction. *Chem. Res. Toxicol.* **2006**, *19*, 539−546.

(46) Paramore, A.; Frantz, S. Bortezomib. *Nat. Rev. Drug Discov.* **2003**, *2*, 611−612.

(47) Larkin, J. D.; Bhat, K. L.; Markham, G. D.; Brooks, B. R.; Schaefer, H. F. III; Bock, C. W. Structure of the boronic acid dimer and the relative stabilities of its conformers. *J. Phys. Chem. A* **2006**, *110*, 10633−10642.

(48) McKee, M. L. Ab initio study of diborane hydrolysis. *J. Phys. Chem.* **1996**, *100*, 8260−8267.

(49) Lindquist, R. N.; Nguyen, A. C. Aminomethaneboronic acids. Synthesis and inhibition of boron analogue of esterase substrates. *J. Am. Chem. Soc.* **1977**, *99*, 6435−6437.

(50) Amssoms, B. K.; Oza, S. L.; Ravaschino, E.; Yamani, A.; Lambeir, A.; Rajan, P.; Bal, G.; Rodriguez, J.; Fairlamb, A. H.; Augustyns, K.; Haemers, A. Glutathione-like tripeptides as inhibitors of glutathionylspermidine synthetase. Part 1: Substitution of the glycine carboxylic acid group. *Bioorg. Med. Chem. Lett.* **2002**, *12*, 2553−2556.

(51) Matteson, D. S.; Sadhu, K. M.; Lienhard, G. E. R-1-Acetamido-2-phenylethaneboronic adic. A specific transition-state analog for chymotrypsin. *J. Am. Chem. Soc.* **1981**, *103*, 5241−5242.

(52) Amiri, P.; Lindquist, R. N.; Matteson, D. S.; Sadhu, K. M. Benzamidomethaneboronic acid: synthesis and inhibition of chymotrypsin. *Arch. Biochem. Biophys.* **1984**, *234*, 531−536.

(53) Duncan, K.; Faraci, W. S.; Matteson, D. S.; Walsh, C. T. (1-Aminoethyl)boronic acid: a novel inhibitor for Bacillus stearothermophilus alanine racemase and Salmonella typhimurium D-alanine:D-alanine ligase (ADP-forming). *Biochemistry* **1989**, *28*, 3541−3549.

(54) Matteson, D. S.; Sadhu, K. M. Synthesis of 1-amino-2-phenylethane-1-boronic acid derivatives. *Organometalllics* **1984**, *3*, 614−618.

(55) Wityak, J.; Earl, R. A.; Abelman, M. M.; Bethel, Y. B.; Fisher, B. N.; Kauffman, G. S.; Kettner, C. A.; Ma, J. L.; McMillan, J. L.; Mersinger, L. J.; Pesti, J.; Pierce, M. E.; Rankin, F. W.; Chorvat, R. J.; Confalone, P. N. Synthesis of thrombin inhibitor DuP714. *J. Org. Chem.* **1995**, *60*, 3717−3722.

(56) Laplante, C.; Hall, D. G. Direct mono-N-methylation of solid-supported amino acids: a useful application of the Matteson rearrangement of alpha-aminoalkylboronic esters. *Organic Letters* **2001**, *3*, 1487−1490.

(57) Matteson, D. S. *Organomet. Chem. Rev.* **1966**, *1*, 1.

(58) Matteson, D. S. *Stereodirected Synthesis with Organoboranes*; Springer: Berlin, 1995.

(59) Matteson, D. S.; Majumdar, D. Iodomethaneboronic esters and aminomethaneboronic esters. *J. Organomet. Chem.* **1979**, *170*, 259−264.

(60) Brooks, M. A.; Scott, L. T. 1,2-Shifts of hydrogen atoms in aryl radicals. *J. Am. Chem. Soc.* **1999**, *121*, 5444−5449.

(61) Kaneti, J. A complete active space self-consistent field (CASSCF) study of the reaction mechanism of the alpha-alkynone rearrangement. *Helv. Chim. Acta* **2000**, *83*, 836−842.

(62) Lewis, F. D.; Sajimon, M. C.; Zuo, X.; Rubin, M.; Gevorgyan, V. Competitive 1,2- and 1.5-hydrogen shifts following 2-vinylbiphenyl photocyclization. *J. Org. Chem.* **2005**, *70*, 10447−10452.

(63) Pachuau, Z.; Lyngdon, R. H. D. Molecular orbital studies on the Wagner-Meerwein migration in some acyclic pinacol-pinacolone rearrangements. *J. Chem. Sci.* **2004**, *116*, 83−91.

(64) Whitmore, F. C. The common basis of intramolecular rearrangements. *J. Am. Chem. Soc.* **1932**, *54*, 3274−3283.

(65) Møller, C.; Pesset, M. S. Note on an approximation treatment for many-electron systems. *Pure Appl. Chem.* **1934**, *46*, 618−622.

(66) Cizek, J. Use of the cluster expansion and the technique of diagrams in calculations of correlation effects in atoms and molecules. *Adv. Chem. Phys.* **1969**, *14*, 35−89.

(67) Purvis, G. D., III; Bartlett, R. J. A full coupled-cluster singles and doubles model: the inclusion of disconnected triples. *J. Chem. Phys.* **1982**, *76*, 1910−1918.

(68) Scuseria, G. E.; Janssen, C. L.; Schaefer, H. F., III An efficient reformulation of the closed-shell coupled cluster single and double excitation (CCSD) equations. *J. Chem. Phys.* **1988**, *89*, 7382−7387.

(69) Scuseria, G. E.; Schaefer, H. F., III Is coupled cluster singles and doubles (CCSD) more computationally intensive than quadratic configuration interaction (QCISD)? *J. Chem. Phys.* **1989**, *90*, 3700−3703.

(70) Krishnan, R.; Binkley, J. S.; Seeger, R.; Pople, J. A. Self-consistent molecular orbital methods. XX. A basis set for correlated wave functions. *J. Chem. Phys.* **1980**, *72*, 650−654.

(71) Clark, T.; Chandrasekhar, J.; Spitznagel, G. W.; Von Ragué Schleyer, P. Efficient diffuse function-augmented basis sets for anion calculations. III. The 3−21+G basis set for first-row elements, Li-F. *J. Comput. Chem.* **2004**, *4*, 294−301.

(72) Dunning, T. H. Jr. Gaussian basis sets for use in correlated molecular calculations. I. The atoms boron through neon and hydrogen. *J. Chem. Phys.* **1989**, *90*, 1007−1023.

(73) Woon, D. E.; Dunning, T. H. Jr. Gaussian basis sets for use in correlated molecular calculations. III. The atoms aluminum through argon. *J. Chem. Phys.* **1993**, *98*, 1358−1371.

(74) Kendall, R. A.; Dunning, T. H. Jr.; Harrison, R. J. Electron affinities of the first-row atoms revisited. Systematic basis sets and wave functions. *J. Chem. Phys.* **1992**, *96*, 6796−6806.

(75) Peterson, K. A.; Woon, D. E.; Dunning, T. H. Jr. Benchmark calculations with correlated molecular wave functions. IV. The classical barrier height of the $H+H_2$ -> H_2+H reaction. *J. Chem. Phys.* **1994**, *100*, 7410−7415.

(76) Frisch, M. J.; Trucks, G. W.; Schlegel, H. B.; Scuseria, G. E.; Robb, M. A.; Cheeseman, J. R.; Montgomery, J. A. Jr.; Vreven, T.; Kudin, K. N.; Burant, J. C.; Millam, J. M.; Iyengar, S. S.; Tomasi, J.; Barone, V.; Mennucci, B.; Cossi, M.; Scalmani, G.; Rega, N.; Petersson, G. A.; Nakatsuji, H.; Hada, M.; Ehara, M.; Toyota, K.; Fukuda, R.; Hasegawa, J.; Ishida, M.; Naskajima, T.; Honda, Y.; Kitao, O.; Nakai, H.; Klene, M.; Li, X.; Knox, J. E.; Hratchian, H. P.; Cross, J. B.; Adamo, C.; Jaramillo, J.; Gomperts, R.; Stratmann, R. E.; Yazyev, O.; Austin, A. J.; Cammi, R.; Pomelli, C.; Ochterski, J. W.; Ayala, P. Y.; Morokuma, K.; Voth, G. A.; Salvador, P.; Dannenberg, J. J.; Zakrzewski, V. G.; Dapprich, S.; Daniels, A. D.; Strain, M. C.; Farkas, O.; Malick, D. K.; Rabuck, A. D.; Raghavachari, K.; Foresman, J. B.; Ortiz, J. V.; Cui, Q.;Baboul, A. G.; Clifford, S.; Cioslowski, J.;Stefanov, B. B.; Liu, G.; Liashenko, A.; Piskorz, P.; Komaromi, I.; Martin, R. L.; Fox, D. J.; Keith, T.; Al-Laham, M. A.;

Peng, C. Y.; Nanayakkara, A.; Challacombe, M.; Gill, P. M. G.; Johnson, B.; Chen, W.; Wong, M. W.; Gonzalez, C.; Pople, J. A. *Gaussian*, I. B.02, R. 2003; Gaussian, Inc.: Pittsburgh, PA, 2003.

(77) Perdew, J. P.; Burke, K.; Ernzerhof, M. Generalized gradient approximation made simple. *Phys. Rev. Lett.* **1996**, *77*, 3865−3868.

(78) Perdew, J. P.; Burke, K.; Ernzerhof, M. Errata-Generalized gradient approximation made simple. *Phys. Rev. Lett.* **1997**, *78*, 1396.

(79) Rabuck, A. D.; Scuseria, G. E. Assessment of recently developed density functionals for the calculation of enthalpies of formation in challenging cases. *Chem. Phys. Lett.* **1999**, *309*, 450−456.

(80) Bhat, K. L.; Braz, V.; Laverty, E.; Bock, C. W. The effectiveness of a primary aliphatic amino group as an internal Lewis base on the formation of a boron-oxygen-carbon linkage: a computational study. *J. Mol. Struct. (THEOCHEM*) **2004**, *712*, 9−19.

(81) Bhat, K. L.; Hakik, S.; Carvo, J. N.; Marycz, D. M.; Bock, C. W. A computational study of the formation of 1,3,2-dioxaborolane from the reaction of dihydroxy borane with 1,2-ethanediol. *J. Mol. Struct. (THEOCHEM*) **2004**, *673*, 145−154.

(82) Bhat, K. L.; Howard, N. J.; Rostami, H.; Lai, J. H.; Bock, C. W. Intramolecular dative bonds involving boron with oxygen and nitrogen in boronic acids and esters: a computational study. *J. Mol. Struct. (THEOCHEM*) **2005**, *723*, 147−157.

(83) Cances, E.; Mennucci, B.; Tomasi, J. A new integral equation formalism for the polarizable continuum model: theoretical background and applications to isotropic and anisotropic dielectrics. *J. Chem. Phys.* **1997**, *1007*, 3032−3041.

(84) Mennucci, B.; Cances, E.; Tomasi, J. Evaluation of solvent effects in isotropic and anisotropic dielectrics and in ionic solutions with a unified integral equation method: theoretical bases, computational implementation, and numerical applications. *J. Phys. Chem. B* **1997**, *101*, 10506−10517.

(85) Mennucci, B.; Tomasi, J. Continuum solvation models: A new approach to the problem of solute's charge distribution and cavity boundaries. *J. Chem. Phys.* **1997**, *106*, 5151−5158.

(86) Cossi, M.; Barone, V.; Mennucci, B.; Tomasi, J. *Ab initio* study of ionic solutions by a polarizable continuum dielectric model. *Chem. Phys. Lett.* **1998**, *286*, 253−260.

(87) Cossi, M.; Scalmani, G.; Rega, N.; Barone, V. New developments in the polarizable continuum model for quantum mechanical and classical calculations on molecules in solution. *J. Chem. Phys.* **2002**, *117*, 43−54.

(88) Tomasi, J.; Mennucci, B.; Cammi, R. Quantum mechanical continuum solvation models. *Chem. Rev.* **2005**, *105*, 2999−3093.

(89) Brooks, B. R. Personal communication, 2006.

(90) Castejon, H.; Wiberg, K. B. Solvent effects on methyl transfer reactions. 1. The Menshutkin reaction. *J. Am. Chem. Soc.* **1999**, *121*, 2139−2146.

(91) Castejon, H.; Wiberg, K. B.; Sklenak, S.; Hinz, W. Solvent effects on methyl transfer reactions. 2. The reaction of amines with trimethylsulfonium salts. *J. Am. Chem. Soc.* **2001**, *123*, 6092−6097.

(92) Kawashima, Y.; Takeo, H.; Matsumura, C. Microwave spectroscopic detection of BFHOH and BH(OH)2. *Chem. Phys. Lett.* **1978**, *57*, 145−147.

(93) Kawashima, Y.; Takeo, H.; Matsumura, C. Microwave spectrum of borinic acid BH_2OH. *J. Chem. Phys.* **1981**, *74*, 5430−5435.

(94) Rettig, S. J.; Trotter, J. Crystal and molecular structure of phenylboronic acid $C_6H_5B(OH)_2$. *Can. J. Chem.* **1977**, *55*, 3071−3075.

(95) Saygili, N.; Batsanov, A. S.; Bryce, M. R. 5-Pyrimidylboronic acid and 2-methoxy-5-pyrimidylboronic acid: new heteroarylpyrimidine derivatives via Suzuki cross-coupling reactions. *Org. Biomol. Chem.* **2004**, *2*, 852−857.

(96) Soundararajan, S.; Duesler, E. N.; Hageman, J. H. Structure of 4-carboxy-2-nitrobenzeneboronic acid. *Acta Crystallogr., Sect. C* **1993**, *49*, 690−693.

(97) Bock, C. W. Unpublished results, 2006.

(98) Matteson, D. S. Functional group compatibilities in boronic ester chemistry. *J. Organomet. Chem.* **1999**, *581*, 51−65.

(99) The role of the amine group in this mechanism appears to be rather minimal; e.g., the corresponding transition state for the protodeboronation of $CH_3-B(OH)_2$ is 35.9 kcal/mol above the separated reactants at the PBE1PBE/6-311++G(d,p) level. It is also worth pointing out that the corresponding transition state for the analogous borane molecule, $H_2N-CH_2-BH_2$, is only 13.2 kcal/mol higher in energy than the separated reactants, although it is 37.1 kcal/mol higher in energy than a $H_2N-CH_2-BH_2\cdots H_2O$ adduct.

(100) A direct protodeboronation mechanism of $H_2N-CH_2-B(OH)_2$ using two explicit water molecules was also investigated. The water molecules were initially positioned to be part of a six-membered ring to facilitate the proton transfer. The Zwitterionic transition state that emerged from the PBE1PBE/6-311++G(d,p) calculation involved H_3O^+ and $B(OH)^-_3$ entities.

(101) deMeijere, A.; Faber, D.; Heinecke, U.; Walsh, R.; Müller, T.; Apeloig, Y. On the question of cyclopropylidene intermediates in cyclopropene-to-allene rearrangements-tegrakis(trimethylsilyl)cyclopropene, 3-alkenyl-1,2,3-tris(trimethylsilyl)cyclopropenes, and related model compounds. *Eur. J. Org. Chem.* **2001**, 663−680.

(102) Höpfl, H. The tetrahedral character of the boron atom newly defined-a useful tool to evaluate the N → B bond. *J. Organomet. Chem.* 1999, *581*, 129−149.

(103) Vidovic, D.; Moore, J. A.; Jones, J. N.; Cowley, A. H. Synthesis and characterization of a coordinated oxoborane: Lewis acid stabilization of a boron-oxygen double bond. *J. Am. Chem. Soc.* **2005**, *127*, 4566−4567.

(104) Calculations on the Zwitterionic structure $H_3C-NH_2-B(OH)(=O)$, in the absence of any explicit water molecules, showed that it was a local minimum; the boron-oxygen distances were 1.26, 1.27 and 1.28 Å at the PBE1PBE/6-311++G(d,p), MP2/cc-pVDZ, and MP2/aug-cc-pVDZ levels respectively, and NBO analyses confirmed the presence of a boron-oxygen double bond.

(105) At the PBE1PBE/6-311++G(d,p) level, no such transition state could be found; several attempts yielded structures similar to transition state **7b** in Figure 2. This is one of the few instances that we have found some significant discrepancy between predictions at the PBE1PBE/6-311++G(d,p) and MP2/aug-cc-pvdz levels.

(106) One possible mechanism that involved a second explicit water molecule in the reaction of intermediate 10 was investigated. A transition state that connects a doubly-hydrated $H_3C-NH_2-B(OH)(=O)$ adduct to a mono-hydrated, dative-bonded $H_3C-H_2N:B(OH)_3$ adduct was located. This transition state was computed to be 12.9 and 8.4 kcal/mol higher in energy than separated 10 and a water molecule.

(107) Chen, X.; Liang, G.; Whitmire, D.; Bowen, J. P. *Ab initio* and molecular mechanics (MM3) calculations on alkyl- and arylboronic acids. *J. Phys. Org. Chem.* **1998**, *11*, 378−386.

(108) Fisher, L.; Holme, T. MM3 parameterization for the B-N bond. *J. Comput. Chem.* **2001**, *22*, 913−922.

(109) James, J. J., Whiting, A. Force field parameters for the boronate function and their carbonyl complexes and application to modeling boronate esters. *J. Chem. Soc., Perkin Trans.* **1996**, *2*, 1861−1867.

(110) Otkidach, D. S.; Pletnev, I. V. Conformtional analysis of boron-containing compounds using Gillespie-Kepert version of molecular mechanics. *J. Mol. Struct. (THEOCHEM)* **2001**, *536*, 65−72.